Germ Granules Coordinate RNA-based Epigenetic Inheritance Pathways

Anne E. Dodson, **Scott Kennedy**[1],[*]

Department of Genetics, Harvard Medical School, Boston, MA 02115, USA

Summary:

Germ granules are biomolecular condensates that promote germ cell totipotency in animals. In *C. elegans*, MEG-3 and MEG-4 function redundantly to assemble germ granules in germline blastomeres. Here, we show that *meg-3/4* mutant animals exhibit defects in RNA interference (RNAi) that are transgenerationally disconnected from the *meg-3/4* genotype. Similar non-Mendelian inheritance is associated with other mutations disrupting germ granule formation, indicating that loss of germ granules is the likely cause of the observed disconnects between genotype and phenotype. *meg-3/4* animals produce aberrant siRNAs that are propagated for ≅10 generations in wild-type descendants of *meg-3/4* ancestors. Aberrant siRNAs inappropriately and heritably silence germline-expressed genes including the RNAi gene *sid-1*, suggesting that transgenerational silencing of *sid-1* underlies inherited defects in RNAi. We conclude that one function of germ granules is to organize RNA-based epigenetic inheritance pathways and that germ granule loss has consequences that persist for many generations.
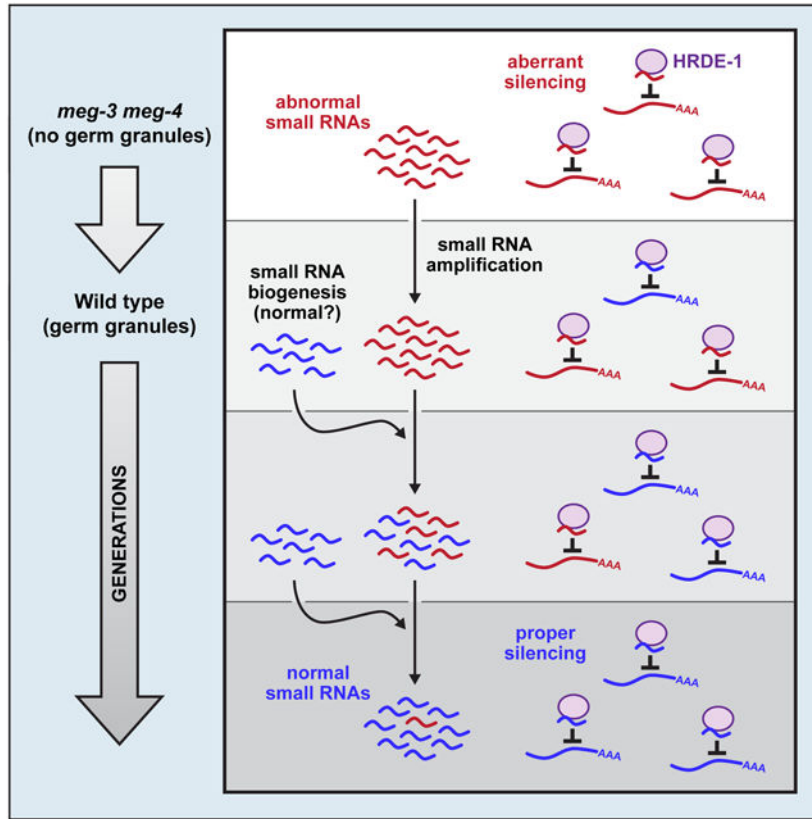
Graphical Abstract

[*]Correspondence: kennedy@genetics.med.harvard.edu.

Declaration of Interests: The authors declare no competing interests.

eTOC blurb

Parentally deposited small non-coding RNAs direct heritable gene regulation in the *C. elegans* germline. Dodson and Kennedy provide evidence that biomolecular condensates known as germ granules spatially organize these small RNA-based epigenetic inheritance pathways. Disrupting germ granules triggers changes in small-RNA-based gene regulation that can be inherited across generations.

Introduction:

Cells contain many non-membrane-bound organelles (termed liquid droplet organelles or biomolecular condensates) that consist of proteins and RNAs that self-assemble via liquid-liquid phase separations (Shin & Brangwynne 2017). Examples of biomolecular condensates include nucleoli, processing (P) bodies, Cajal bodies, stress granules, neuronal granules, and germ granules (Shin & Brangwynne 2017). Germ granules are biomolecular condensates that form in the germ cells of many metazoans to help maintain totipotency of the germline (Voronina et al. 2011). The mechanism(s) by which germ granules promote germ cell health are largely unknown (Voronina et al. 2011; Voronina 2013). According to current models, one major function of biomolecular condensates such as germ granules may be to bring specific proteins and nucleic acids together in space and time to help organize the complex RNA processing pathways underlying gene regulation (Toretsky & Wright 2014; Weber & Brangwynne 2012).

Germ granules in *C. elegans* (referred to as P granules) are present in germ cells during all stages of development (Strome & Wood 1983). During early embryonic cell divisions, P granules assemble asymmetrically in the germline-destined portion of the zygotic cytoplasm (Brangwynne et al. 2009). MEG-3 and MEG-4 are intrinsically disordered proteins that are expressed during early embryogenesis and that function redundantly to nucleate P granule formation in early embryos (Wang et al. 2014; Smith et al. 2016). Another protein, DEPS-1, contributes to P granule formation during most stages of germline development (Spike et al. 2008). For much of development, P granules localize to the outer nuclear membrane directly adjacent to nuclear pores. Multiple lines of evidence suggest that P granules help surveil and/or process mRNAs as they transit through nuclear pores and enter the cytoplasm (Pitt et al. 2000; Sheth et al. 2010). For example, newly synthesized mRNAs have been observed transiting P granules (Sheth et al. 2010), and specific mRNAs concentrate in P granules during specific stages of germline development (Seydoux & Fire 1994). Additionally, a number of RNA quality control proteins, including small RNA pathway components, localize to P granules (see below). Finally, in the absence of P granules, somatic genes become improperly expressed in the germline (Updike et al. 2014; Knutson et al. 2017). Thus, P granules likely function to store and surveil mRNAs in germ cells.

Non-coding RNAs, such as PIWI-interacting RNAs (piRNAs) and endogenous small interfering RNAs (endo-siRNAs), contribute to RNA quality control in many eukaryotes and, in some cases, also transmit epigenetic information from parent to progeny (Boškovi & Rando 2018). In *C. elegans*, many instances of transgenerational epigenetic inheritance (TEI) are directed by endo-siRNAs (Rechavi & Lev 2017). Current models posit that, during TEI, endo-siRNAs are deposited into the embryo via the egg or sperm. Parentally deposited endo-siRNAs then act as guide molecules to identify cognate mRNAs, recruit RNA-dependent RNA Polymerases (RdRPs), and amplify endo-siRNA populations. Repetition of this process each new generation allows endo-siRNA-based gene regulatory information to pass across multiple generations. Heritably maintained endo-siRNA populations bind Argonaute proteins such as HRDE-1 to regulate gene expression in germ cells (Buckley et al. 2012; Shirayama et al. 2012). Many of the genomic loci targeted for heritable silencing by endo-siRNAs in *C. elegans* are pseudogenes and cryptic loci, suggesting that the endo-siRNA system may have evolved to silence unwanted germline RNAs (Gu et al. 2009). This heritable gene regulatory pathway is likely important for germ cell function, as mutations that disrupt this process also cause a germline mortal (Mrt) phenotype in which germ cell function deteriorates over generations (Buckley et al. 2012; Spracklin et al. 2017; Wan et al. 2018). In summary, *C. elegans* possess an RNA-based mode of epigenetic inheritance driven by generationally repeated amplification of endo-siRNAs by RdRPs, followed by silencing of unwanted RNAs by germline-expressed Argonautes such as HRDE-1.

Because endo-siRNA-based gene regulation is both complex and heritable, it is likely that cells regulate and organize endo-siRNA biogenesis in ways that prevent runaway heritable silencing of the wrong mRNAs. P granules may provide this organization, as many endo-siRNA pathway proteins are known to localize to P granules, including the RNase III enzyme Dicer, the Dicer-related factor DRH-3, the endo-siRNA-binding Argonautes WAGO-1 and CSR-1, the piRNA-binding Argonaute PRG-1, and the RdRP EGO-1 (Claycomb et al. 2009; Batista et al. 2008; Beshore et al. 2011; Gu et al. 2009). Other endo-

siRNA pathway factors localize to other germline biomolecular condensates (WAGO-4 and ZNFX-1 in Z granules and RRF-1 in *Mutator* foci) that form ordered multi-condensate structures with P granules in adult *C. elegans* germ cells (Wan et al. 2018; Phillips et al. 2012). Together, the data hint that various *C. elegans* germ granules may act as organizational hubs that help connect endo-siRNA pathway proteins with the correct mRNAs to help ensure fidelity and accuracy of endo-siRNA-based gene regulation.

Here, we show that mutations that disrupt germ granule formation trigger the production of aberrant endo-siRNAs that inappropriately silence germline-expressed genes. Due to the heritable nature of endo-siRNAs, aberrations in gene expression are inherited across multiple generations, even after germ granules have been restored. We conclude that one function of germ granules is to organize and coordinate RNA-based epigenetic inheritance pathways and that the loss of this organizational function has consequences that can persist for many generations.

Results:

meg-3/4 animals exhibit defects in experimental RNAi.

RNA interference (RNAi) can be triggered experimentally in *C. elegans* by feeding animals bacteria that express dsRNAs targeting specific *C. elegans* mRNA sequences (referred to hereinafter as experimental RNAi) (Timmons et al. 2001). Mutations in *deps-1* disrupt P granule formation in adult *C. elegans* germ cells and also lead to defects in experimental RNAi, suggesting that P granules may contribute in some way to small RNA-based gene regulation in germ cells (Spike et al. 2008). To further investigate a potential link between P granules and germline small RNA pathways, we asked if other mutations that affect P granule formation also cause defects in experimental RNAi. MEG-3 and MEG-4 (together, MEG-3/4) are two intrinsically disordered proteins that are redundantly required for P granule assembly during early embryogenesis, but not during larval development or in the adult germline (Wang et al. 2014; Smith et al. 2016). *tm4259* and *ax2026* are putative null alleles of *meg-3* and *meg-4,* respectively (Wang et al. 2014; Mitani 2009). RNAi targeting either *pos-1* or *egg-4/5,* which are essential germline genes, causes sterility in *C. elegans* (Fig. 1A and Fig. S1A) (Parry et al. 2009). *meg-3(tm4259) meg-4(ax2026)* animals remained fertile after either *pos-1* RNAi or *egg-5* RNAi, suggesting that MEG-3/4 are required for experimental RNAi in germ cells (Fig. 1A). *meg-3(tm4259) meg-4(ax2026)* animals also failed to silence a germline-expressed *gfp* reporter gene after exposure to *gfp* RNAi, confirming that MEG-3/4 contribute to RNAi-based gene silencing in germ cells (Fig. S1B). *meg-3(tm4259) meg-4(ax2026)* animals responded normally to RNAi targeting genes expressed in the soma, suggesting that the role of MEG-3/4 in promoting experimental RNAi may be restricted to the germline (Fig. S1C) (Wan et al. 2018). *ax3055* and *ax3052* are independently isolated deletion alleles of *meg-3* and *meg-4*, respectively (Smith et al. 2016). Similar to *meg-3(tm4259) meg-4(ax2026)* animals, *meg-3(ax3055) meg-4(ax3052)* animals responded normally to RNAi targeting somatically expressed genes, but failed to respond to RNAi targeting the germline-expressed *pos-1* and *egg-4/5* genes (Fig. 1A and Fig. S1A,C). The data show that MEG-3/4 contribute to dsRNA-based gene silencing in the

germline and thereby support the idea that P granule formation is somehow important for dsRNA-based gene silencing.

Transgenerational disconnect between *meg-3/4* genotype and phenotype.

While conducting genetic crosses and RNAi experiments with *meg-3(tm4259) meg-4(ax2026)* animals (henceforth, *meg-3/4*), we noticed that the RNAi-defective (Rde) phenotype associated with *meg-3/4* was transgenerationally disconnected from the *meg-3/4* genotype. For instance, the *meg-3/4* offspring of heterozygous (++*/meg-3/4*) parents surprisingly responded to *pos-1* RNAi (Fig. 1B). Amazingly, descendants of these newly generated *meg-3/4* mutants did not become Rde until MEG-3/4 function had been absent for 5–9 generations (Fig. 1B). [Note: for reasons that will become apparent below, the ++*/ meg-3/4* parents of the animals described above were maintained as heterozygotes for >20 generations prior to isolation of *meg-3/4* homozygous progeny in these experiments.] PGL-1 is a commonly used marker of P granules, and PGL-1 fails to concentrate into the germline blastomeres of MEG-3/4(−) embryos (Wang et al. 2014; Smith et al. 2016). To ensure that MEG-3/4 function was lost in the *meg-3/4* animals described above, we monitored the subcellular localization of a PGL-1::RFP fluorescent marker protein in the various offspring of ++*/meg-3/4* parents. We found that PGL-1::RFP concentrated properly in wild-type and ++*/meg-3/4* embryos, but not in *meg-3/4* embryos (Fig. 1C). Importantly, the *meg-3/4* progeny in this experiment responded normally to RNAi, even though these animals did not possess detectable embryonic P granules (Fig. S1D). Thus, MEG-3/4 function is transgenerationally disconnected from Rde phenotypes. The fact that *meg-3/4* animals do not become Rde for many generations after the loss of MEG-3/4 indicates that MEG-3/4 do not play a direct role in dsRNA-based gene silencing. Rather, loss of MEG-3/4 triggers a process that indirectly impairs RNAi over many generations. Henceforth, we use the term "phenotypic lag" to refer to situations where a phenotype does not appear for many generations after genotype is established.

Ancestral loss of P granules is associated with phenotypic hangovers.

Outcrossing *meg-3/4* animals to wild type revealed a second type of transgenerational disconnect between *meg-3/4* genotype and phenotype. When *meg-3/4* animals were crossed to wild-type males, both the wild-type and *meg-3/4* F_2 progeny of the cross were Rde (Fig. 2A,B). Amazingly, lineages established from the wild-type progeny of *meg-3/4* ancestors remained defective for *pos-1* RNAi for 9–11 generations before eventually reverting to a wild-type phenotype (Fig. 2B). Control crosses between wild type and wild type did not produce progeny exhibiting RNAi defects (Fig. 2A,B). Wild-type lineages derived from the *meg-3/4* outcross were also defective for RNAi targeting *egg-4/5* for >10 generations (Fig. S2A). Interestingly, putting wild-type descendants under strong selection for inheriting Rde (by maintaining lines on *egg-5* RNAi) did not prolong the generational perdurance of the Rde phenotype (Fig. S2A). When a different set of *meg-3/4* alleles, *meg-3(ax3055)* and *meg-4(ax3052)*, were outcrossed, two out of three crosses also produced wild-type descendants that were RNAi-defective for multiple generations (Fig. S2B). Offspring from the third cross did not show an Rde phenotype (Fig. S2B), which may be related to the observation that a small percentage (approximately 5–10%) of *meg-3(ax3055) meg-4(ax3052)* individuals do not exhibit an Rde phenotype (see Fig. 1A and Fig. S1A). The

fact that wild-type descendants of *meg-3/4* animals typically retain an Rde phenotype for many generations indicates that mechanisms unrelated to *meg-3/4* genotype exist to propagate the Rde phenotype across generations. Henceforth, we use the term "phenotypic hangover" to refer to the transgenerational inheritance of a phenotype in the absence of the mutant genotype that originally triggered the phenotype. The remainder of this paper investigates the mechanism underlying *meg-3/4*-associated phenotypic hangovers.

Phenotypic hangovers are likely initiated by failure to assemble P granules.

MEG-3/4 nucleate P granule assembly in germline blastomeres (Wang et al. 2014; Smith et al. 2016). We wondered if the Rde hangovers associated with loss of MEG-3/4 might be related to the role of MEG-3/4 in P granule assembly. DEPS-1 is a *C. elegans* protein that 1) localizes to P granules, 2) is partially required for P granule assembly (primarily in adult germ cells), and 3) contributes to experimental RNAi in the germline (Spike et al. 2008). To test our model that P granule disruption causes Rde hangovers, we asked whether mutations in *deps-1* could, like *meg-3/4*, trigger Rde hangovers. We crossed *deps-1(bn124)* animals to wild-type males, isolated homozygous wild-type or homozygous *deps-1* progeny, and measured RNAi responsiveness in lineages established from these animals. Both wild-type and mutant progeny of *deps-1(bn124)* ancestors were Rde, and lineages established from the wild-type progeny of *deps-1(bn124)* ancestors remained Rde for 2–5 generations after they had become genetically wild-type for *deps-1* (Fig. 2C). RDE-4 is a dsRNA-binding protein that is thought to play a direct role in dsRNA-mediated gene silencing by working with Dicer to process dsRNAs into siRNAs (Tabara et al. 2002). RDE-4 has no known role in P granule assembly. Unlike *meg-3/4* or *deps-1* outcrosses, *rde-4* outcrosses showed Mendelian inheritance of the Rde phenotype, indicating that (as expected) not all RNAi-related factors are associated with Rde hangovers (Fig. 2D). Altogether, our data suggest that Rde hangovers are likely triggered by an ancestral loss of P granules.

The inheritance phase of Rde hangovers is not associated with obvious defects in germ granule morphology or localization.

We wondered if Rde hangovers might be caused by inherited defects in P granule assembly. To test this idea, we first generated animals that were homozygous mutant for *meg-3/4* and that expressed PGL-1::RFP, a fluorescent marker of P granules (Wan et al. 2018). We next outcrossed *pgl-1::rfp; meg-3/4* animals (after animals had been *meg-3/4* mutants for $\cong$10 generations) to *pgl-1::rfp; meg-3/4(+)* males and monitored PGL-1::RFP subcellular localization in embryos in the uteri of F_2 progeny from this cross. Whereas embryonic P granules failed to concentrate properly in *meg-3/4* homozygous progeny, as expected, embryonic P granules formed properly in animals that had just become wild-type for *meg-3/4* (Fig. 3A). P granules also appeared normal in the adult germline in wild-type F_2 progeny (Fig. S3A). We conclude that, although Rde hangovers are likely initiated by the loss of P granules, the maintenance of Rde hangovers is not associated with the inheritance of obvious defects in P granule morphology or localization.

hrde-1 suppresses the Rde phenotype associated with *meg-3/4* animals.

Small RNAs are major vectors for transgenerational epigenetic inheritance (TEI) in plants and animals. Current models posit that, during endo-siRNA-directed TEI in *C. elegans*, a

bolus of endo-siRNAs is deposited into the embryo via the egg or sperm. Parentally deposited endo-siRNAs then act as guide molecules to identify cognate mRNAs and recruit RdRP enzymes, which then amplify endo-siRNA populations. Finally, repetition of this process each generation allows gene regulatory information to pass across multiple generations. The germline-expressed Argonaute HRDE-1 is, for unknown reasons, required for endo-siRNA-directed TEI in *C. elegans* (Buckley et al. 2012; Ashe et al. 2012; Shirayama et al. 2012; Luteijn et al. 2012). To ask if endo-siRNA-based TEI might somehow underlie Rde hangovers, we tested whether the Rde phenotype associated with *meg-3/4* animals depended on HRDE-1. Indeed, *tm1200*, a deletion allele of *hrde-1*, suppressed the RNAi defect, but not the P granule defect, associated with *meg-3/4* animals (Fig. 3B and Fig. S3B). HRDE-1 acts with Nuclear RNAi Defective-2 (NRDE-2) to drive endo-siRNA-based TEI (Guang et al. 2010; Buckley et al. 2012). NRDE-2 was also required for *meg-3/4* animals to exhibit an Rde phenotype (Fig. 3B). These data support the idea that endo-siRNA-directed TEI contributes in some way to the RNAi defect associated with *meg-3/4* animals.

MEG-3/4 help organize endo-siRNA pathways.

How might the endo-siRNA system contribute to RNAi defects and Rde hangovers? A number of endo-siRNA pathway factors localize to P granules (see Introduction). Thus, P granules may bring specific Argonautes, RdRPs, and mRNAs together in space and time in ways that help produce the correct numbers and types of endo-siRNAs each generation. This idea led us to the following model that might explain the mechanistic underpinnings of Rde hangovers. First, the disruption of P granules, via mutations like *meg-3/4* or *deps-1*, disorganizes endo-siRNA pathways, leading to aberrant production of endo-siRNAs targeting one or more genes required for RNAi (termed *RNAi gene-x* genes). Second, disorganized endo-siRNAs propagate across generations to transgenerationally silence *RNAi gene-x* (via HRDE-1), resulting in an Rde hangover. Note: for this model to work, *RNAi gene-x* would need to contribute to experimental RNAi, but not endo-siRNA-based TEI. To test our model, we sequenced small RNAs (≅15–30 nucleotides) using a 5′-phosphate-independent cloning method capable of sequencing *C. elegans* endo-siRNAs (see Method Details). We sequenced small RNAs from replicates of wild-type and *meg-3/4* animals, as well as genetically wild-type animals whose ancestors had been *meg-3/4* 3–25 generations prior to sequencing. Reads were mapped to the *C. elegans* genome, and the number of small RNAs mapping antisense to each *C. elegans* gene was quantified. We searched for genes that were differentially targeted by small RNAs in wild-type and *meg-3/4* animals (adjusted p-value < 0.05 and log2 fold change > 1 or < −1). The analysis identified 94 and 396 genes that were targeted by more or fewer small RNAs, respectively, in *meg-3/4* animals than in wild-type animals (termed MEG-3/4-regulated genes) (Fig. 3C and Table S1). Small RNAs targeting MEG-3/4-regulated genes were mostly 22 nucleotides in length, and the majority of 22-nucleotide RNAs initiated with guanosine (Fig. S3C). Given that such features are hallmarks of endo-siRNAs, we henceforth refer to these small RNAs as MEG-3/4-regulated endo-siRNAs (Billi et al. 2014). Although the number of MEG-3/4-regulated endo-siRNAs went up or down in *meg-3/4* animals on a gene-by-gene basis, the total number of endo-siRNAs targeting all MEG-3/4-regulated genes remained similar in wild-type and *meg-3/4* animals (Fig. 3D). Thus, loss of MEG-3/4 alters the degree to which some genes are targeted

by endo-siRNAs, but does not have a major effect on the overall number of endo-siRNAs produced. Previous studies have sub-categorized *C. elegans* endo-siRNAs into two major groups: endo-siRNAs associated with the Worm-specific Argonautes (WAGOs), and endo-siRNAs associated with the Argonaute CSR-1 (Claycomb et al. 2009; Gu et al. 2009). MEG-3/4-regulated endo-siRNAs were largely WAGO-class endo-siRNAs ($p < 0.0001$) (Fig. 3E). WAGO-class endo-siRNAs engage a number of WAGO-class Argonautes, including HRDE-1, to regulate gene expression (Billi et al. 2014). MEG-3/4-regulated endo-siRNAs were enriched for HRDE-1-interacting endo-siRNAs ($p < 0.0001$) (Fig. 3E) (Buckley et al. 2012). Therefore, loss of MEG-3/4 and embryonic P granules is associated with aberrant levels of WAGO-class, HRDE-1-associated endo-siRNAs.

Wild-type descendants of *meg-3/4* animals inherit aberrant endo-siRNA populations.

Our model predicts that disruptions to endo-siRNA populations should persist in genetically wild-type descendants of *meg-3/4* animals for the duration of Rde hangovers (approximately ten generations). We therefore analyzed levels of MEG-3/4-regulated endo-siRNAs across generations in wild-type descendants of *meg-3/4* animals. Hierarchical clustering using the complete linkage method revealed three discernable patterns of inheritance (Fig. 4A). Most endo-siRNAs that were abundant in *meg-3/4* animals relative to the wild-type control remained high in the initial generations of the Rde hangover and then diminished to wild-type control levels over the course of 25 generations (Class 1 in Fig. 4A). Endo-siRNAs that were reduced in *meg-3/4* animals relative to the wild-type control fell into two major categories: a) endo-siRNAs that remained low in the initial generations of the hangover and increased slowly, many of which never fully recovered to wild-type control levels by the F_{25} generation (Class 2 in Fig. 4A); and b) endo-siRNAs that remained low in the initial generations of the hangover but recovered relatively quickly (Class 3 in Fig. 4A). Hierarchical clustering using divisive analysis also identified discrete patterns of endo-siRNA inheritance that resemble the categories described above (Fig. S4A). Both clustering analyses showed that the majority of MEG-3/4-regulated endo-siRNA pools progressed from mutant-like levels to wild-type levels over the course of 25 generations. A small proportion of MEG-3/4-regulated endo-siRNAs deviated from this general pattern of inheritance. For example, 6 pools of heritable endo-siRNAs remained at mutant-like levels for 25 generations and showed little evidence of reversion to wild-type levels (Fig. S4B). *hrde-1* affected the levels of 4 of these 6 endo-siRNA pools, suggesting that this remarkably stable inheritance was epigenetic (and not genetic) in nature (see Discussion). Interestingly, many aberrant endo-siRNA pools were unaffected by *hrde-1* in a *meg-3/4* mutant background, yet were still inherited in wild-type descendants of *meg-3/4* animals (Fig. S4C,D). Thus, HRDE-1-independent mechanisms of inheritance may exist in *C. elegans*.

The analyses described above indicate that aberrant endo-siRNA populations are inherited over many generations in animals whose ancestors lacked P granules. To further understand this remarkable pattern of inheritance, we subjected our sequencing data to principal component analysis (PCA). Briefly, PCA identifies and ranks sources of variation (termed principal components, or PCs) between datasets and then shows how the datasets relate to one another with regard to each PC. In the case of our small RNA sequencing data, for example, samples with similar small RNA profiles should cluster together in a plot of the

highest-ranking PCs. PCA of our small RNA sequencing data revealed that the largest source of variation, PC1, corresponds to genotype, with *meg-3/4* animals and wild type exhibiting the least similarity (Fig. 4B). Interestingly, wild-type descendants of *meg-3/4* animals dispersed along the PC1 axis by generation: earlier generations more closely resembled *meg-3/4* animals, whereas later generations more closely resembled wild type, providing further evidence that wild-type descendants of *meg-3/4* animals evolve over the course of many generations from a mutant-like state to a wild-type state (Fig. 4B). PCA also revealed that, in each generation, biological replicates cluster together (Fig. 4B). Therefore, even though the recovery of endo-siRNA pools may take many generations, this process is reproducible and, therefore, largely deterministic.

Ancestral loss of P granules is associated with heritable silencing of RNAi genes.

Our model also predicts that aberrant endo-siRNA populations should inappropriately silence genes needed for experimental RNAi. Indeed, two of the top 12 most significantly upregulated endo-siRNA pools mapped to genes with known roles in experimental RNAi in *C. elegans* (*sid-1* and *rde-11*) (Fig. 3C and Table S1). SID-1 is a putative transmembrane protein that is expressed in the soma and germline, where it is thought to act as a channel for transporting dsRNA into cells (Feinberg & Hunter 2003; Winston et al. 2002; Shih & Hunter 2011). RDE-11 is a zinc finger protein that is thought to function in the amplification step of RNAi (Yang et al. 2012; Zhang et al. 2012). *sid-1* and *rde-11* endo-siRNAs were elevated 9-fold and 13-fold in *meg-3/4* mutant animals, respectively, and remained elevated in wild-type descendants of *meg-3/4* animals for approximately 10 generations (Fig. 5A,B and Fig. S5). Thus, the generational kinetics of Rde hangovers and aberrant *sid-1/rde-11* endo-siRNA inheritance are quite similar. To determine the effects of these endo-siRNAs on gene expression, we used quantitative RT-PCR to measure the levels of *sid-1* and *rde-11* mRNA. *sid-1* and *rde-11* mRNA levels were down 5-fold and 6-fold in *meg-3/4* animals, respectively, and remained low in wild-type descendants of *meg-3/4* animals for approximately 10 generations (Fig. 5B and Fig. S5B). Heritable downregulation of *sid-1/rde-11* expression therefore also correlates with Rde hangovers. The data hint that runaway silencing of *sid-1* or *rde-11* (or both) may be responsible for *meg-3/4*-associated Rde hangovers. Since the RNAi defect associated with *meg-3/4* depends on HRDE-1, we asked whether the misregulation of *sid-1/rde-11* in *meg-3/4* animals also depends on HRDE-1. Indeed, *hrde-1* suppressed both the increased levels of *sid-1/rde-11* endo-siRNAs and the decreased levels of *sid-1/rde-11* mRNAs observed in *meg-3/4* animals (Fig. 5A,B and Fig. S5). Previous studies have shown that HRDE-1 interacts with endo-siRNAs targeting *sid-1* and *rde-11*, suggesting that the role of HRDE-1 in *sid-1/rde-11* silencing is likely to be direct (Buckley et al. 2012). Thus, HRDE-1 promotes both *sid-1/rde-11* silencing and germline Rde in the absence of MEG-3/4, and likely propagates these defects in wild-type animals whose ancestors lacked MEG-3/4. We conclude that ancestral loss of P granules is associated with heritable defects in gene expression, and that defects specific to *sid-1* and/or *rde-11* may be the cause of Rde hangovers.

rde-11 and *sid-1* mutants respond idiosyncratically to dsRNAs injected directly into the germline (Zhang et al. 2012; Winston et al. 2002; Wang & Hunter 2017). For instance, *rde-11* mutants show a partial RNAi defect in response to low doses of injected dsRNA (0.5

ng/ul), but respond normally to high doses of injected dsRNA (20 ng/ul or 200 ng/ul) (Zhang et al. 2012). This differential sensitivity may be due to the presumed role of RDE-11 in amplifying gene silencing signals (Zhang et al. 2012; Yang et al. 2012). *sid-1* mutants, on the other hand, are sensitive to the number of gonad arms injected with dsRNA (the *C. elegans* germline is comprised of two distinct gonad arms) (Winston et al. 2002; Wang & Hunter 2017). Because *C. elegans* RNAi is systemic (capable of spreading between tissues), dsRNA injection into a single gonad arm (or the soma) can trigger gene silencing in the germ cells of both gonad arms in wild-type animals (Fig. 5C) (Fire et al. 1998). However, in *sid-1* mutants, which are defective for systemic RNAi, dsRNA injection only triggers gene silencing in the injected gonad and this silencing fails to spread to the other gonad arm (Winston et al. 2002; Wang & Hunter 2017). We took advantage of these observations to ask if aberrant silencing of *rde-11* or *sid-1* might be the cause of Rde hangovers: We injected *meg-3/4* with a high dose of *pos-1* dsRNA (200 ng/ul) and asked if *meg-3/4* animals either 1) behaved like *rde-11* mutants (responded like wild-type to a high dose of dsRNAs), or 2) behaved like *sid-1* mutants (responded more robustly to injection of both gonad arms vs. a single arm). *meg-3/4* animals exhibited an Rde phenotype following injection of 200 ng/ul of *pos-1* dsRNA into either one or two gonad arms, suggesting that aberrant *rde-11* silencing is not solely responsible for the Rde phenotype of *meg-3/4* animals (Fig. 5C). Injecting both gonad arms of *meg-3/4* animals triggered more robust gene silencing than injection of a single gonad arm (Fig. 5C). *sid-1* mutant animals behaved similarly to *meg-3/4* animals in this assay (Fig. 5C). By contrast, *rde-1* mutant animals, which are fully defective for autonomous RNAi (Tabara et al. 1999), failed to respond to dsRNA injection regardless of the number of gonad arms injected (Fig. 5C). The data suggest that the RNAi defect associated with *meg-3/4* is largely systemic in nature. Thus, the data are consistent with a model in which the Rde phenotype associated with *meg-3/4* is caused by aberrant silencing of the *sid-1* gene. Note: for this model to be correct, aberrant silencing of the *sid-1* gene would need to be limited to germ cells, as *sid-1* mutant animals, but not *meg-3/4* mutant animals, exhibit RNAi defects in the soma (Fig. S1C) (Winston et al. 2002).

Discussion:

Here, we show that mutations disrupting P granules trigger phenotypes that are transgenerationally disconnected from genotype. Disconnects correlate with alterations in endogenous small RNA levels and gene expression patterns, which persist across generations in the wild-type descendants of animals that lacked P granules. The data suggest that one function of germ granules is to organize and coordinate RNA-based modes of epigenetic inheritance. Upon loss of this germ granule-based organization, epigenetic defects are propagated on a generational timescale.

We find that MEG-3/4 regulate the degree to which particular genes are targeted by endo-siRNAs. How might MEG-3/4 (and therefore embryonic P granules) regulate endo-siRNA pathways? A subset of maternally deposited mRNAs and endo-siRNA pathway proteins (e.g. EGO-1, PRG-1, CSR-1, and WAGO-1) localize to P granules (Seydoux & Fire 1994; Vought et al. 2005; Claycomb et al. 2009; Batista et al. 2008; Gu et al. 2009). Thus, one function of P granules may be to spatially organize endo-siRNA biogenesis by ensuring that endo-siRNA pathway factors interact only with the proper mRNA targets (Fig. 5D). Such

organization may be necessary to prevent the endo-siRNA system, which is inherently dangerous due to its feed-forward and heritable nature, from targeting functionally important germline genes for runaway heritable silencing. We propose that, in the absence of the organizing capabilities of P granules, one or more small RNA pathway factors fails to connect with its correct mRNA targets, resulting in over-targeting of some mRNAs and under-targeting of other mRNAs (Fig. 5D). In this issue of *Developmental Cell*, Ouyang *et al.*, 2019 report that P granules limit piRNA-based gene silencing. The piRNA-binding Argonaute PRG-1, which directs the production of endo-siRNAs bound by HRDE-1 (Ashe et al. 2012; de Albuquerque et al. 2015; Phillips et al. 2015), is required for the RNAi defect and aberrant gene silencing that occurs in *meg-3/4* animals (Ouyang et al., 2019, this issue of *Developmental Cell*). In support of an organizational role for P granules, MEG-3/4 regulate the localization of both PRG-1 and specific mRNAs that become mis-targeted for silencing in *meg-3/4* animals (Ouyang et al., 2019, this issue of *Developmental Cell*).

Because endo-siRNAs can be inherited, aberrant endo-siRNAs produced in the absence of P granules propagate for many generations, even after P granules have been restored. We find that wild-type descendants of *meg-3/4* ancestors can inherit aberrant endo-siRNA and mRNA patterns for over 25 generations. The fact that most endo-siRNA pools eventually return to wild-type levels (and do so reproducibly in biological replicates) indicates that, although recovery may take many generations, it is still largely a deterministic process. Thus, the information that ultimately dictates which mRNAs should and should not be channeled into the endo-siRNA pathway is likely hardwired in the genome. This hardwiring likely involves piRNAs, which are genomically encoded small RNAs with the ability to initiate endo-siRNA biogenesis in *C. elegans* (Ruby et al. 2006; Batista et al. 2008; Das et al. 2008; Gu et al. 2009). Interestingly, we also find that some changes in endo-siRNA pools triggered by the loss of embryonic P granules were stably inherited for at least 25 generations. Epigenetic inheritance at these loci may represent situations in which endo-siRNA-based inheritance is so efficient that it has become largely divorced from genetic/piRNA control. Finally, we also identified a number of MEG-3/4-regulated endo-siRNA pools that were unaffected by *hrde-1*, hinting that HRDE-1-independent mechanisms for small RNA-based TEI may exist in *C. elegans*.

Our data argue against a direct role for embryonic P granules in experimental RNAi, as we have documented multiple examples of a) animals that lack embryonic P granules but respond normally to germline RNAi, and b) animals that possess P granules but fail to respond to germline RNAi. How, then, might *meg-3/4* mutations impair RNAi? A likely explanation is that the loss of P granules in *meg-3/4* triggers the production of endo-siRNAs that inappropriately and heritably silence one or more genes required for experimental RNAi in the germline (Fig. 5E). Multiple lines of evidence support this idea. First, *meg-3/4* animals produce abnormally high levels of endo-siRNAs that inappropriately silence *sid-1* and *rde-11*, two genes required for experimental RNAi. Second, aberrant levels of *sid-1/rde-11* endo-siRNAs and aberrant silencing of *sid-1/rde-11* mRNA are inherited for approximately 10 generations and, therefore, occur concomitantly with Rde hangovers. Third, aberrant *sid-1/rde-11* silencing and the *meg-3/4* RNAi defect both depend on the same factor: HRDE-1. Lastly, our dsRNA injection data point specifically to *sid-1* as the gene whose aberrant silencing triggers Rde hangovers, as *meg-3/4* mutant animals show a

systemic defect in germline RNAi that mimics that of *sid-1* mutant animals. For the above reasons, we speculate that inappropriate and heritable silencing of the *sid-1* locus in germ cells is the cause of Rde hangovers. Proving this model will require additional work, which could include experimentally restoring *sid-1* expression to wild-type levels in animals undergoing Rde hangovers. A related model might explain the phenotypic lags we observe in *meg-3/4* animals. Specifically, loss of P granules (via introduction of *meg-3/4* mutations) might cause a small increase in *sid-1* endo-siRNAs that, initially, is not sufficient to effectively silence *sid-1*. In subsequent generations, however, *sid-1* endo-siRNAs would originate from two sources: 1) continued mild overproduction of endo-siRNAs (due to the absence of P granules), and 2) parental deposition of endo-siRNAs that were produced in previous generations. According to this model, over four to five generations, *sid-1* endo-siRNAs would accumulate to levels sufficient to silence the *sid-1* locus (Fig. 5E). Sequencing endo-siRNAs during a *meg-3/4* phenotypic lag would be a strong test of this idea.

In addition to *sid-1* and *rde-11*, hundreds of other genes are also mistargeted by aberrant endo-siRNAs in the wild-type descendants of *meg-3/4* animals (Fig. 4). It is possible that inappropriate silencing of these genes could trigger additional types of phenotypic lags or hangovers that have not yet been documented. Furthermore, mutations disrupting germ granule assembly or organization at other developmental time points might trigger a distinct set of genotype/phenotype disconnects, as the types of mRNAs that would be available to inappropriately enter the endo-siRNA pathway would likely change throughout development. Supporting this idea, some of the genes misregulated in *deps-1* animals (which exhibit defects in P granule assembly in both embryos and adult germ cells) were also identified by us in *meg-3/4* animals (which lack embryonic P granules), whereas other regulated genes were unique to each genotype (Table S2) (Spike et al. 2008). Notably, *deps-1* mutations decrease the expression of *rde-4*, a gene required for RNAi; therefore, reduced levels of RDE-4 (and not SID-1) may underlie the germline RNAi defect of *deps-1* mutants (Spike et al. 2008).

C. elegans possess a robust mode of TEI thought to transmit an RNA-based memory of germline gene expression programs from parent to progeny. We find that perturbing this mode of TEI (by disrupting P granule formation) leads to heritable defects in germline gene expression programs. Given that systems exist to transmit epigenetic information across generations, it stands to reason that genetic or environmental perturbations that alter the quality or quantity of this information would have heritable effects, even if the initiating perturbation were short-lived. Although heritable alterations to the epigenome could conceivably be adaptive, it is more likely that such changes would have negative impacts on organismal fitness, which could persist for generations. Such considerations may also apply to other modes of TEI and other animals, as mutations affecting chromatin or gene regulatory factors in both *C. elegans* and mammals have also been linked to phenotypic hangovers (Greer et al. 2011; Nelson et al. 2012; Siklenka et al. 2015). Given that many genes, pathways, and environmental signals are likely to impinge upon the germline epigenome, phenotypic lags and phenotypic hangovers, such as those documented here, may turn out to be a fairly common phenomenon. Exploring how much phenotypic variation is contingent upon ancestral genotype, assessing the generational perdurance of this type of

variation in different animals, and asking if phenotypic hangovers ever contribute to disease inheritance in humans will be important questions for future studies to address.

STAR Methods:

Lead Contact and Materials Availability

Further information and requests for resources and reagents should be directed to and will be fulfilled by the Lead Contact, Scott Kennedy (kennedy@genetics.med.harvard.edu). Strains are available upon request from the authors.

Experimental Model and Subject Details

C. elegans were grown at 20°C for all experiments. Unless otherwise indicated, animals were maintained on Nematode Growth Medium (NGM) plates seeded with *E. coli* OP50. Genetic crosses described in this study were between hermaphrodites and males. Phenotypic analyses were performed on hermaphrodites. A list of strains used in this study can be found in the Key Resources Table.

Method Details

Bacteria-mediated RNA interference: Animals were fed *E. coli* HT115 expressing dsRNAs targeting the indicated genes. *E. coli* HT115 containing the L4440 vector was used as a no-RNAi control in Figure 1A, Figure 3B, and Figure S1. RNAi clones, with the exception of *gfp* RNAi, were obtained from the Ahringer *C. elegans* RNAi library (Kamath et al. 2003). For tests using *pos-1* RNAi or *egg-5* RNAi, RNAi feeding began at the L2/L3 larval stages. *gfp* RNAi feeding began at the L3 larval stage, and *gfp* silencing was scored in the same generation at the adult stage. Somatic RNAi assays were performed by plating embryos onto bacteria expressing the indicated dsRNAs, and silencing was scored in the same generation at the adult stage. Details on scoring and sample size are described in figure legends.

Phenotypic lag experiments: The *dpy-3* locus is approximately 0.1 cM from *meg-3* and 0.8 cM from *meg-4* (*meg-3* and *meg-4* are approximately 0.7 cM apart). We first marked a *meg-3(tm4259) meg-4(ax2026)* chromosome with *dpy-3(e27)*. Then, we crossed *meg-3(tm4259) meg-4(ax2026) dpy-3(e27)* animals to wild-type males and maintained a *meg-3(tm4259) meg-4(ax2026) dpy-3(e27)* chromosome in a heterozygous state for at least 22 generations. Multiple independent lines were established in this manner. Every generation, non-Dpy progeny were singled from non-Dpy parents that gave rise to both Dpy and non-Dpy progeny. Prior to performing lag experiments, lines were genotyped for *meg-3* and *meg-4* by PCR to check whether *meg-3(tm4259)* and *meg-4(ax2026)* were still linked to *dpy-3(e27)*. The progeny of animals that had been heterozygous for 22 generations were singled, tested for sensitivity to *pos-1* RNAi, and then genotyped for *meg-3* and *meg-4* by PCR (n = 72). In parallel, siblings of the progeny tested for RNAi were singled under normal growth conditions, genotyped for *meg-3* and *meg-4* by PCR, and wild-type and *meg-3/4* animals were used to establish lines (6 wild-type lines and 10 *meg-3/4* lines). Lines were maintained under normal growth conditions. Every subsequent generation, a small pool of animals (3–5) from each line was tested for sensitivity to *pos-1* RNAi. Lines were re-

genotyped for *meg-3* and *meg-4* approximately every 5 generations. As a control, *meg-3(tm4259) meg-4(ax2026) dpy-3(e27)* animals were crossed to *meg-3(tm4259) meg-4(ax2026)* males, and the *dpy-3(e27)* allele was maintained in a heterozygous state for at least 22 generations, whereas *meg-3(tm4259)* and *meg-4(ax2026)* were maintained in a homozygous state. Fifteen *meg-3(tm4259) meg-4(ax2026) dpy-3(e27)* lines were then established and tested in parallel with the lines described in the first cross. To examine the P granule phenotype of newly generated *meg-3/4* mutants (Fig. 1C), similar crosses were performed as described above, except animals also contained *pgl-1(gg547[pgl-1::3xflag::tagrfp])* to mark P granules and *mjIs31[pie-1p::gfp::h2b]* to mark chromatin. For this experiment, *meg-3/4* genotype was inferred from the Dpy phenotype.

Phenotypic hangover experiments: In general, hangover experiments began by crossing animals homozygous for the mutant allele(s) of interest [e.g. *meg-3(tm4259) meg-4(ax2026)*] to wild-type males (P_0 generation). Multiple independent crosses were performed for each experiment. In the F_2 generation, L2/L3 larvae were singled, tested for sensitivity to *pos-1* (or *egg-5*) RNAi, and then genotyped by PCR. Siblings of those animals were singled under normal growth conditions, genotyped by PCR, and were then used to establish either homozygous wild-type or homozygous mutant lines. Unless otherwise indicated, lines were maintained under normal growth conditions for the duration of the experiment. Each subsequent generation, a small pool of animals (3–5) from each line was tested for sensitivity to *pos-1* (or *egg-5*) RNAi. Lines were re-genotyped by PCR every 5–10 generations. As a control, wild-type animals descending from a cross between wild-type hermaphrodites and wild-type males were tested for sensitivity to *pos-1* (or *egg-5*) RNAi in parallel with the wild-type descendants of mutant animals. To examine the P granule phenotype in wild-type descendants of *meg-3(tm4259) meg-4(ax2026)* animals (Fig. 3A and Fig. S3A), similar crosses were performed as described above, except animals also contained *pgl-1(gg547[pgl-1::3xflag::tagrfp])* to mark P granules and *mjIs31[pie-1p::gfp::h2b]* to mark chromatin. In addition, the *meg-3(tm4259) meg-4(ax2026)* chromosome was marked with *dpy-3(e27)*, and *meg-3/4* genotype was inferred from the Dpy phenotype.

Sample collection for small RNA-seq and qRT-PCR: The following crosses were performed in parallel in preparation for RNA isolation: 1) *meg-3(tm4259) meg-4(ax2026)* animals were crossed to wild-type males (P_0 generation), and wild-type descendants of this cross were collected in generations F_3 through F_7, F_{10}, F_{15}, and F_{25}; and 2) as a control, wild-type animals were crossed to wild-type males (P_0 generation), and the descendants of this cross, which were all wild type, were collected in generation F_3 (this sample is referred to as the wild-type control). For each type of cross, biological replicates were derived from different parents (P_0s). To amass enough animals for RNA isolation, 30–50 wild-type lines were established in the F_2 generation (for each biological replicate), and lines were pooled starting in the F_3 generation. *meg-3(tm4259) meg-4(ax2026)* animals that had been homozygous mutant for dozens of generations were collected as a mutant control. Approximately 10% of *meg-3(tm4259) meg-4(ax2026)* animals do not develop a full germline, and 27% of *meg-3(tm4259) meg-4(ax2026)* animals are sterile (have empty uteri) (Wang et al. 2014). To help control for the proportion of germ cells in each sample, adults with empty uteri were removed with a standard worm pick prior to sample collection. Adult

worms were washed two times with M9 Buffer, resuspended and vortexed for 30 seconds in TRIzol, then flash-frozen in liquid nitrogen and stored at −80°C. Total RNA was isolated by TRIzol extraction.

Small RNA library preparation and sequencing: RNAs ranging from approximately 15 to 30 nucleotides were gel-purified from total RNA (20 ug) on a 15% polyacrylamide/urea gel and then ligated to a 3' adapter using T4 RNA ligase 2, truncated (New England BioLabs). To enable the cloning of 5'-triphosphorylated RNAs, samples were treated with Antarctic Phosphatase (New England BioLabs) followed by treatment with T4 polynucleotide kinase (New England BioLabs) as described previously (Gent et al. 2009). Prior to ligation of the 5' adapter, 3'-ligated small RNAs and any excess 3' adapter were hybridized to the oligo that would eventually be used as a primer for reverse transcription. This step was taken to help minimize adapter-dimer formation (McReynolds & Munafo 2014). To help avoid cross-contamination, the 5' adapter was modified to contain the Illumina genomic sequencing primer annealing site followed by an additional 4 nucleotides at the 3' end. Two different 5' adapters (ending in either AGCG or CGUC) were mixed in a 1:1 ratio, and the mix was ligated to each sample using T4 RNA ligase I (New England BioLabs). Every sample was treated with the same mix of 5' adapters. Libraries were amplified and multiplexed with a 6-nucleotide 3' barcode, then pooled for next-generation sequencing on a NextSeq500 (Biopolymers Facility, HMS).

Computational analysis of small RNA-seq: First, custom scripts were used to select reads starting with the last 4 nucleotides of the 5' adapters (either AGCG or CGTC). Cutadapt 1.14 was used to trim the 3' adapter (cutadapt -a CTGTAGGCACCATCAATAGATCGGAAGAGCAC -m 14 -- discard-untrimmed) and the in-line portion of the 5' adapter (cutadapt -u 4) (Martin 2011). Trimmed reads were then mapped to the *C. elegans* genome (WormBase release WS260) using Bowtie 1.2.2 (Langmead et al. 2009). No mismatches were allowed. The number of reads mapping antisense to each gene was determined using featureCounts (featureCounts -s 2) (Liao et al. 2014). Raw counts were then normalized by the median of ratios method using DESeq2 1.22.2 in R (Love et al. 2014; RStudio Team 2016). Differential analyses were performed using DESeq2 1.22.2 (Love et al. 2014). To identify MEG-3/4-regulated endo-siRNA pools that did not recover to wild-type levels by the F_{25} generation (Fig. S4B), DESeq2 was used to find genes that were differentially targeted by small RNAs in wild-type F_{25} descendants of *meg-3/4* animals (the last generation of the hangover that was tested) and wild-type control animals (adjusted p-value < 0.05 and log2 fold change > 1 or < −1), and the resulting genes were tested for overlap with the list of MEG-3/4-regulated genes. To identify MEG-3/4-regulated endo-siRNA pools that were unaffected by *hrde-1* (Fig. S4C,D), DESeq2 was used to find genes that were differentially targeted by small RNAs in *meg-3/4* and *hrde-1; meg-3/4* animals (adjusted p-value < 0.05 and log2 fold change > 1 or < −1), and the resulting genes were tested for overlap with the list of MEG-3/4-regulated genes. Heatmaps (Fig. 4A and Fig. S4C) were clustered by row (genes) and scaled by row using pheatmap 1.0.12 in R (Kolde 2015). The gene clusters shown in Figure S4A were generated using DEGreport 1.18.1 in R (Pantano 2019). Principal component analysis of rlog-transformed counts (Fig. 4B) was performed using the rlog and plotPCA functions in

DESeq2 1.22.2 (Love et al. 2014). Custom scripts were used to extract the features of small RNAs that mapped antisense to MEG-3/4-regulated genes. Coverage plots (Fig. 5A and Fig. S5A) were generated as follows: first, bedGraph files normalized by counts per million were produced for the forward and reverse strands using deepTools 3.0.2 (bamCoverage -bs 5 --normalizeUsing CPM --samFlagExclude 16) and (bamCoverage -bs 5 --normalizeUsing CPM --samFlagInclude 16) (Ramírez et al. 2016); then, bedGraph files were plotted in R using Sushi 1.20.0 (Phanstiel et al. 2014).

Quantitative RT-PCR: Using the total RNA prepared as described above, mRNA was reverse-transcribed into cDNA using the SuperScript III First-Strand Synthesis System (Invitrogen). Quantitative RT-PCR was performed with the iTaq Universal SYBR Green Supermix (Bio-Rad) and the primers listed in the Key Resources Table. Cycle threshold values were calibrated to a standard curve generated using a 4-point, 1:2 dilution series of wild-type control cDNA. PCR reactions were performed in technical triplicate for each biological replicate.

Microscopy: Animals were immobilized in M9 Buffer containing 0.05% sodium azide and mounted on glass slides. Images were taken with a wide-field Zeiss Axio Observer.Z1 microscope equipped with an ORCA-Flash 4.0 CMOS camera (Hamamatsu) and the following Zeiss objectives: Plan-Apochromat 63×/1.4 Oil DIC M27, Plan-Apochromat 20×/0.8 M27, and EC Plan-Neofluar 10×/0.3 Ph1 M27. Embryos were imaged *in utero*. Images were acquired with ZEN software (Zeiss) and compiled in Fiji (Schindelin et al. 2012).

Synthesis and microinjection of pos-1 dsRNA: *pos-1* dsRNA was synthesized *in vitro* using a MEGAscript T7 Transcription Kit (Invitrogen). The transcription template was PCR-amplified from the Ahringer *pos-1* RNAi clone and contained the *pos-1* insert sequence as well as the flanking T7 promoters. *pos-1* dsRNA was injected into one or both gonad arms of young adults at a concentration of 200 ng/ul. At least 9 animals were injected per condition. 18–22 hours post-injection, animals were singled and allowed to lay embryos for approximately 20 hours. Progeny and unhatched eggs were counted 24 hours later. A small fraction of *meg-3/4* animals did not lay eggs and were therefore excluded from the analysis. Mutant alleles were the following: *meg-3(tm4259) meg-4(ax2026)*, *sid-1(qt9)*, and *rde-1(ne219)*.

Quantification and Statistical Analysis

Differential analyses for small RNA sequencing were performed with the Wald test using DESeq2 1.22.2, and genes with both an adjusted p-value < 0.05 and a log2 fold change >1 or < −1 were deemed significant (Love et al. 2014). Significance values reported in the description of Figure 3E were calculated with the one-sided Fisher's exact test using the fisher.test function in R (RStudio Team 2016). Significance values shown in Figure 5C were calculated with the Student's t-test (two-tailed, unequal variances) using Excel. All error bars represent standard deviation. Sample sizes are indicated in the figure legends and Method Details.

Data and Code Availability

The small RNA sequence data generated during this study are available from Gene Expression Omnibus (GEO) under the accession number GEO: GSE134683.

Supplementary Material

Refer to Web version on PubMed Central for supplementary material.

Acknowledgements:

References:

de Albuquerque BFM, Placentino M & Ketting RF, 2015 Maternal piRNAs Are Essential for Germline Development following De Novo Establishment of Endo-siRNAs in Caenorhabditis elegans. Developmental cell, 34(4), pp.448–456. [PubMed: 26279485]

Ashe A et al., 2012 piRNAs can trigger a multigenerational epigenetic memory in the germline of C. elegans. Cell, 150(1), pp.88–99. [PubMed: 22738725]

Batista PJ et al., 2008 PRG-1 and 21U-RNAs interact to form the piRNA complex required for fertility in C. elegans. Molecular cell, 31(1), pp.67–78. [PubMed: 18571452]

Beshore EL et al., 2011 C. elegans Dicer interacts with the P-granule component GLH-1 and both regulate germline RNPs. Developmental biology, 350(2), pp.370–381. [PubMed: 21146518]

Billi AC, Fischer SEJ & Kim JK, 2014 Endogenous RNAi pathways in C. elegans. WormBook: the online review of C. elegans biology, pp.1–49.

Boškovi A & Rando OJ, 2018 Transgenerational Epigenetic Inheritance. Annual review of genetics, 52, pp.21–41.

Brangwynne CP et al., 2009 Germline P granules are liquid droplets that localize by controlled dissolution/condensation. Science, 324(5935), pp.1729–1732. [PubMed: 19460965]

Buckley BA et al., 2012 A nuclear Argonaute promotes multigenerational epigenetic inheritance and germline immortality. Nature, 489(7416), pp.447–451. [PubMed: 22810588]

Claycomb JM et al., 2009 The Argonaute CSR-1 and its 22G-RNA cofactors are required for holocentric chromosome segregation. Cell, 139(1), pp.123–134. [PubMed: 19804758]

Das PP et al., 2008 Piwi and piRNAs act upstream of an endogenous siRNA pathway to suppress Tc3 transposon mobility in the Caenorhabditis elegans germline. Molecular cell, 31(1), pp.79–90. [PubMed: 18571451]

Feinberg EH & Hunter CP, 2003 Transport of dsRNA into cells by the transmembrane protein SID-1. Science, 301(5639), pp.1545–1547. [PubMed: 12970568]

Fire A et al., 1998 Potent and specific genetic interference by double-stranded RNA in Caenorhabditis elegans. Nature, 391(6669), pp.806–811. [PubMed: 9486653]

Gent JI et al., 2009 A Caenorhabditis elegans RNA-directed RNA polymerase in sperm development and endogenous RNA interference. Genetics, 183(4), pp.1297–1314. [PubMed: 19805814]

Greer EL et al., 2011 Transgenerational epigenetic inheritance of longevity in Caenorhabditis elegans. Nature, 479(7373), pp.365–371. [PubMed: 22012258]

Guang S et al., 2010 Small regulatory RNAs inhibit RNA polymerase II during the elongation phase of transcription. Nature, 465(7301), pp.1097–1101. [PubMed: 20543824]

Gu W et al., 2009 Distinct argonaute-mediated 22G-RNA pathways direct genome surveillance in the C. elegans germline. Molecular cell, 36(2), pp.231–244. [PubMed: 19800275]

Kamath RS et al., 2003 Systematic functional analysis of the Caenorhabditis elegans genome using RNAi. Nature, 421(6920), pp.231–237. [PubMed: 12529635]

Knutson AK et al., 2017 Germ Granules Prevent Accumulation of Somatic Transcripts in the Adult Caenorhabditis elegans Germline. Genetics, 206(1), pp.163–178. [PubMed: 28258184]

Kolde R, 2015 Pheatmap: pretty heatmaps.

Langmead B et al., 2009 Ultrafast and memory-efficient alignment of short DNA sequences to the human genome. Genome biology, 10(3), p.R25. [PubMed: 19261174]

Liao Y, Smyth GK & Shi W, 2014 featureCounts: an efficient general purpose program for assigning sequence reads to genomic features. Bioinformatics, 30(7), pp.923–930. [PubMed: 24227677]

Love MI, Huber W & Anders S, 2014 Moderated estimation of fold change and dispersion for RNA-seq data with DESeq2. Genome biology, 15(12), p.550. [PubMed: 25516281]

Luteijn MJ et al., 2012 Extremely stable Piwi-induced gene silencing in Caenorhabditis elegans. The EMBO journal, 31(16), pp.3422–3430. [PubMed: 22850670]

Martin M, 2011 Cutadapt removes adapter sequences from high-throughput sequencing reads. EMBnet.*journal*, 17(1), pp.10–12.

McReynolds LA & Munafo D, 2014 Method for reducing adapter-dimer formation. US Patent. Available at: https://patentimages.storage.googleapis.com/e1/34/e2/e18d15902ac72e/US8883421.pdf.

Mitani S, 2009 Nematode, an experimental animal in the national BioResource project. Experimental animals / Japanese Association for Laboratory Animal Science, 58(4), pp.351–356.

Nelson VR et al., 2012 Transgenerational epigenetic effects of the Apobec1 cytidine deaminase deficiency on testicular germ cell tumor susceptibility and embryonic viability. Proceedings of the National Academy of Sciences of the United States of America, 109(41), pp.E2766–73. [PubMed: 22923694]

Pantano L, 2019 DEGreport: Report of DEG analysis, Available at: http://lpantano.github.io/DEGreport/.

Parry JM et al., 2009 EGG-4 and EGG-5 Link Events of the Oocyte-to-Embryo Transition with Meiotic Progression in C. elegans. Current biology: CB, 19(20), pp.1752–1757. [PubMed: 19879147]

Phanstiel DH et al., 2014 Sushi.R: flexible, quantitative and integrative genomic visualizations for publication-quality multi-panel figures. Bioinformatics, 30(19), pp.2808–2810. [PubMed: 24903420]

Phillips CM et al., 2012 MUT-16 promotes formation of perinuclear mutator foci required for RNA silencing in the C. elegans germline. Genes & development, 26(13), pp.1433–1444. [PubMed: 22713602]

Phillips CM et al., 2015 piRNAs and piRNA-Dependent siRNAs Protect Conserved and Essential C. elegans Genes from Misrouting into the RNAi Pathway. Developmental cell, 34(4), pp.457–465. [PubMed: 26279487]

Pitt JN, Schisa JA & Priess JR, 2000 P granules in the germ cells of Caenorhabditis elegans adults are associated with clusters of nuclear pores and contain RNA. Developmental biology, 219(2), pp.315–333. [PubMed: 10694425]

Ramírez F et al., 2016 deepTools2: a next generation web server for deep-sequencing data analysis. Nucleic acids research, 44(W1), pp.W160–5. [PubMed: 27079975]

Rechavi O & Lev I, 2017 Principles of Transgenerational Small RNA Inheritance in Caenorhabditis elegans. Current biology: CB, 27(14), pp.R720–R730. [PubMed: 28743023]

RStudio Team, 2016 RStudio: Integrated Development for R.

Ruby JG et al., 2006 Large-scale sequencing reveals 21U-RNAs and additional microRNAs and endogenous siRNAs in C. elegans. Cell, 127(6), pp.1193–1207. [PubMed: 17174894]

Schindelin J et al., 2012 Fiji: an open-source platform for biological-image analysis. Nature methods, 9(7), pp.676–682. [PubMed: 22743772]

Seydoux G & Fire A, 1994 Soma-germline asymmetry in the distributions of embryonic RNAs in Caenorhabditis elegans. Development, 120(10), pp.2823–2834. [PubMed: 7607073]

Sheth U et al., 2010 Perinuclear P granules are the principal sites of mRNA export in adult C. elegans germ cells. Development, 137(8), pp.1305–1314. [PubMed: 20223759]

Shih JD & Hunter CP, 2011 SID-1 is a dsRNA-selective dsRNA-gated channel. RNA, 17(6), pp.1057–1065. [PubMed: 21474576]

Shin Y & Brangwynne CP, 2017 Liquid phase condensation in cell physiology and disease. Science, 357(6357).

Shirayama M et al., 2012 piRNAs Initiate an Epigenetic Memory of Nonself RNA in the C. elegans Germline. Cell, 150(1), pp.65–77. [PubMed: 22738726]

Siklenka K et al., 2015 Disruption of histone methylation in developing sperm impairs offspring health transgenerationally. Science, 350(6261), p.aab2006. [PubMed: 26449473]

Smith J et al., 2016 Spatial patterning of P granules by RNA-induced phase separation of the intrinsically-disordered protein MEG-3. eLife, 5.

Spike CA et al., 2008 DEPS-1 promotes P-granule assembly and RNA interference in C. elegans germ cells. Development, 135(5), pp.983–993. [PubMed: 18234720]

Spracklin G et al., 2017 Identification and Characterization of Caenorhabditis elegans RNAi Inheritance Machinery. Genetics, p.genetics.116.198812.

Strome S & Wood WB, 1983 Generation of asymmetry and segregation of germ-line granules in early C. elegans embryos. Cell, 35(1), pp.15–25. [PubMed: 6684994]

Tabara H et al., 2002 The dsRNA binding protein RDE-4 interacts with RDE-1, DCR-1, and a DExH-box helicase to direct RNAi in C. elegans. Cell, 109(7), pp.861–871. [PubMed: 12110183]

Tabara H et al., 1999 The rde-1 gene, RNA interference, and transposon silencing in C. elegans. Cell, 99(2), pp.123–132. [PubMed: 10535731]

Timmons L, Court DL & Fire A, 2001 Ingestion of bacterially expressed dsRNAs can produce specific and potent genetic interference in Caenorhabditis elegans. Gene, 263(1–2), pp.103–112. [PubMed: 11223248]

Toretsky JA & Wright PE, 2014 Assemblages: functional units formed by cellular phase separation. The Journal of cell biology, 206(5), pp.579–588. [PubMed: 25179628]

Updike DL et al., 2014 Germ-granule components prevent somatic development in the C. elegans germline. Current biology: CB, 24(9), pp.970–975. [PubMed: 24746798]

Voronina E et al., 2011 RNA granules in germ cells. Cold Spring Harbor perspectives in biology, 3(12).

Voronina E, 2013 The diverse functions of germline P-granules in Caenorhabditis elegans. Molecular reproduction and development, 80(8), pp.624–631. [PubMed: 23150384]

Vought VE et al., 2005 EGO-1, a putative RNA-directed RNA polymerase, promotes germline proliferation in parallel with GLP-1/notch signaling and regulates the spatial organization of nuclear pore complexes and germline P granules in Caenorhabditis elegans. Genetics, 170(3), pp.1121–1132. [PubMed: 15911573]

Wan G et al., 2018 Spatiotemporal regulation of liquid-like condensates in epigenetic inheritance. Nature, 557(7707), pp.679–683. [PubMed: 29769721]

Wang E & Hunter CP, 2017 SID-1 Functions in Multiple Roles To Support Parental RNAi in Caenorhabditis elegans. Genetics, 207(2), pp.547–557. [PubMed: 28751423]

Wang JT et al., 2014 Regulation of RNA granule dynamics by phosphorylation of serine-rich, intrinsically disordered proteins in C. elegans. eLife, 3, p.e04591. [PubMed: 25535836]

Weber SC & Brangwynne CP, 2012 Getting RNA and protein in phase. Cell, 149(6), pp.1188–1191. [PubMed: 22682242]

Winston WM, Molodowitch C & Hunter CP, 2002 Systemic RNAi in C. elegans requires the putative transmembrane protein SID-1. Science, 295(5564), pp.2456–2459. [PubMed: 11834782]

Yang H et al., 2012 The RDE-10/RDE-11 complex triggers RNAi-induced mRNA degradation by association with target mRNA in C. elegans. Genes & development, 26(8), pp.846–856. [PubMed: 22508728]

Zhang C et al., 2012 The Caenorhabditis elegans RDE-10/RDE-11 complex regulates RNAi by promoting secondary siRNA amplification. Current biology: CB, 22(10), pp.881–890. [PubMed: 22542102]
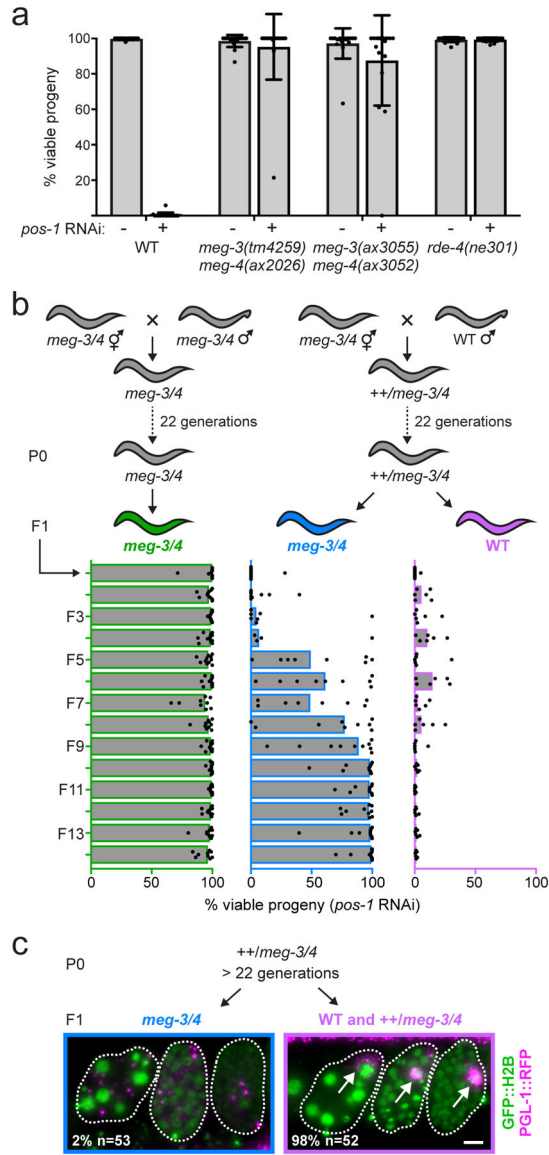
Highlights

- Disrupting germ granules leads to aberrant levels of endogenous small RNAs.

- Aberrantly expressed small RNAs misregulate germline gene expression.

- Gene expression defects caused by germ granule loss are inherited across generations.

Figure 1. Transgenerational disconnect between *meg-3/4* genotype and phenotype.
(a) L2 larvae of the indicated genotypes were fed either bacteria expressing dsRNAs derived from the *pos-1* gene, which is required for embryonic viability, or bacteria containing the control vector, L4440. When the animals became adults, they were allowed to lay broods, and % hatching embryos was scored. Black dots represent individual broods (n = 18). Error bars represent +/− standard deviations of the mean (gray bars). **(b)** Top panel: schematic of genetic crosses. We first marked *meg-3(tm4259) meg-4(ax2026)* with *dpy-3(e27)* (*dpy-3* is 0.1 cM from *meg-3* and 0.8 cM from *meg-4*). Then, *meg-3(tm4259) meg-4(ax2026) dpy-3(e27)* animals were crossed to wild-type males, and heterozygous progeny were identified by PCR-based genotyping of both *meg-3* and *meg-4*. As a mutant control cross, *meg-3(tm4259) meg-4(ax2026) dpy-3(e27)* animals were crossed to *meg-3(tm4259) meg-4(ax2026)* males. Lines that were either homozygous (control cross) or heterozygous for *meg-3/4* mutations were maintained for 22 generations (data presented later in the paper

will clarify why this was necessary for this experiment). All lines remained heterozygous for *dpy-3(e27)*. The progeny of homozygous or heterozygous *meg-3/4* lines were isolated, and *meg-3* and *meg-4* were genotyped by PCR. These progeny were used to establish 6 lineages that were maintained for 14 generations under normal growth conditions. Bottom panel: at the indicated generations, animals from each lineage were exposed to *pos-1* RNAi and % hatching embryos was scored. Black dots represent individual lineages, colored bars represent the median value of % viable progeny. **(c)** A *meg-3(tm4259) meg-4(ax2026) dpy-3(e27)* chromosome was maintained in a heterozygous state for ≅45 generations in animals that were homozygous for two fluorescent protein markers: *pgl-1::rfp* (Wan et al. 2018), which marks P granules (magenta), and *gfp::h2b* (Ashe et al. 2012), which marks chromatin (green). PGL-1::RFP and GFP::H2B were visualized in first-generation *meg-3/4* animals (indicated by Dpy phenotype) and their *meg-3/4(+)* and *++/meg-3/4* siblings (indicated by non-Dpy phenotype). Fluorescent micrographs of three embryos in the uterus of one adult are shown. Arrows indicate P granules. The percentage of F_1 adults containing embryos with normal PGL-1::RFP expression and the number of adults scored are indicated. Scale bar, 10 microns. See also Figure S1.
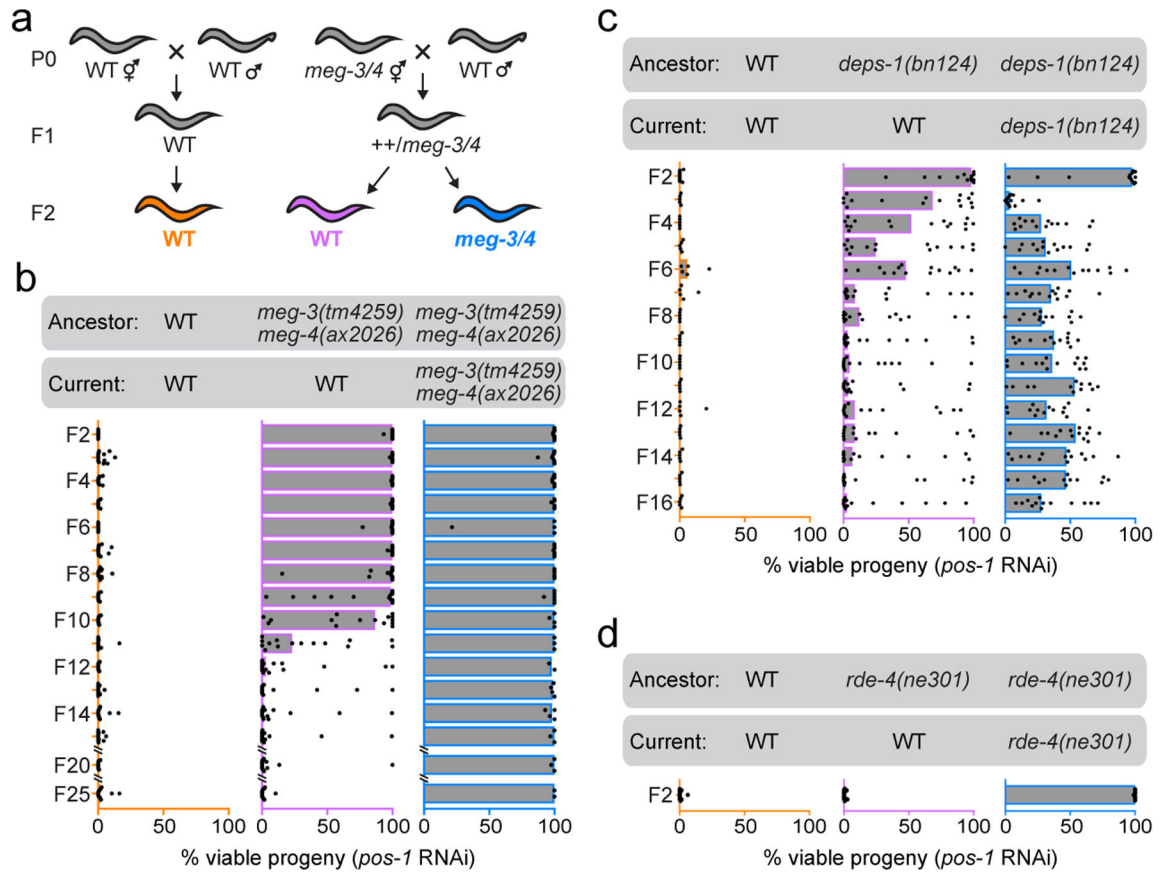
Figure 2. Ancestral loss of P granules is associated with phenotypic hangovers.
(a) Schematic of genetic crosses used to generate animals scored for RNAi responsiveness in
(b). Note: for this experiment, *meg-3(tm4259) meg-4(ax2026)* animals had been maintained
in a homozygous state for dozens of generations prior to outcross. (b) 15 lineages were
established from F_2 progeny and were maintained for 24 generations under normal growth
conditions. At the indicated generations, animals from each lineage were exposed to *pos-1*
RNAi and % hatching embryos was scored. Black dots represent individual lineages, colored
bars represent the median value of % viable progeny. (c) *deps-1(bn124)* animals were
crossed to wild-type males and descendants of the crosses were scored for *pos-1* RNAi
sensitivity as described in (b). (d) *rde-4(ne301)* animals were crossed to wild-type males,
and wild-type and *rde-4* progeny were scored for *pos-1* RNAi sensitivity. See also Figure S2.
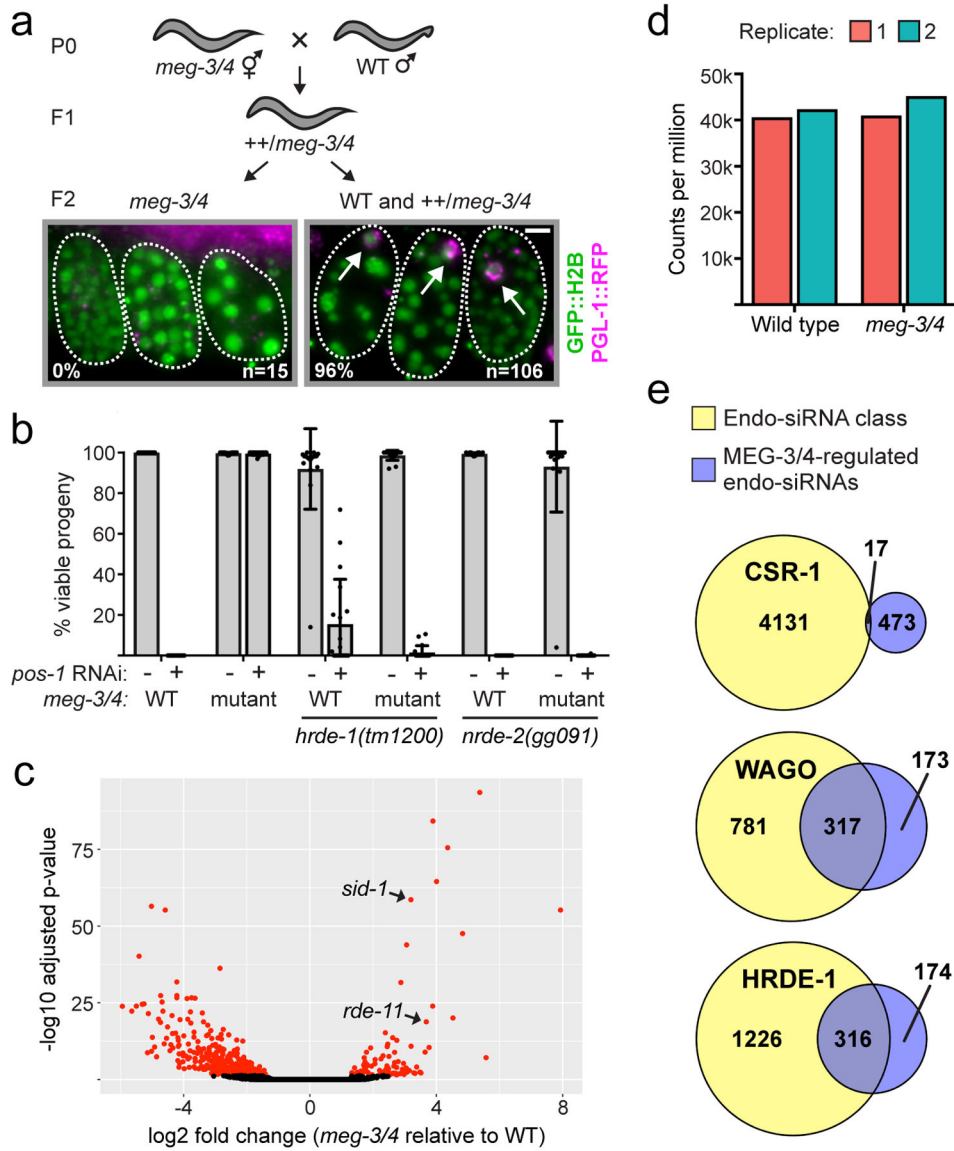
Figure 3. MEG-3/4 help organize endo-siRNA pathways.
(a) *gfp::h2b; pgl-1::rfp; meg-3/4 dpy-3* animals that had been maintained in the homozygous state for dozens of generations were crossed to *gfp::h2b; pgl-1::rfp* males (WT). In the F_2 generation, *meg-3/4(+)* and *++/meg-3/4* adults (indicated by non-Dpy phenotype) or *meg-3/4* homozygous adults (indicated by Dpy phenotype) were imaged. Fluorescent micrographs of three embryos in the uterus of one adult are shown. Arrows indicate P granules. The percentage of F_2 adults containing embryos with normal PGL-1::RFP expression and the number of adults scored are indicated. Scale bar, 10 microns. **(b)** Loss of HRDE-1 or NRDE-2 suppresses the RNAi defect associated with *meg-3/4*. Individual animals of the indicated genotypes were scored for *pos-1* RNAi sensitivity as described in Figure 1A (n = 18). Error bars represent +/− standard deviations of the mean (gray bars). WT, wild type. **(c)** Volcano plot showing log2 fold change in the # of endo-siRNAs targeting each *C. elegans* gene in *meg-3(tm4259) meg-4(ax2026)* animals relative to wild type on the

x-axis and the –log10 adjusted p-value on the y-axis. Dots shown in red indicate endo-siRNA pools that were significantly different between genotypes. *rde-11* and *sid-1* endo-siRNA pools are labeled for reasons that will become clear in Figure 5. **(d)** The number of endo-siRNAs targeting all MEG-3/4-regulated genes normalized to the total number of small RNAs sequenced from each sample are shown for each replicate of wild type and *meg-3/4*. k=1000. **(e)** Overlap between the list of MEG-3/4-regulated genes and published lists of genes targeted by CSR-1-bound endo-siRNAs (Claycomb et al. 2009), genes in the WAGO class (Gu et al. 2009), and genes targeted by HRDE-1-bound endo-siRNAs (Buckley et al. 2012). Numbers of genes overlapping and non-overlapping between lists are indicated. See also Figure S3 and Table S1.
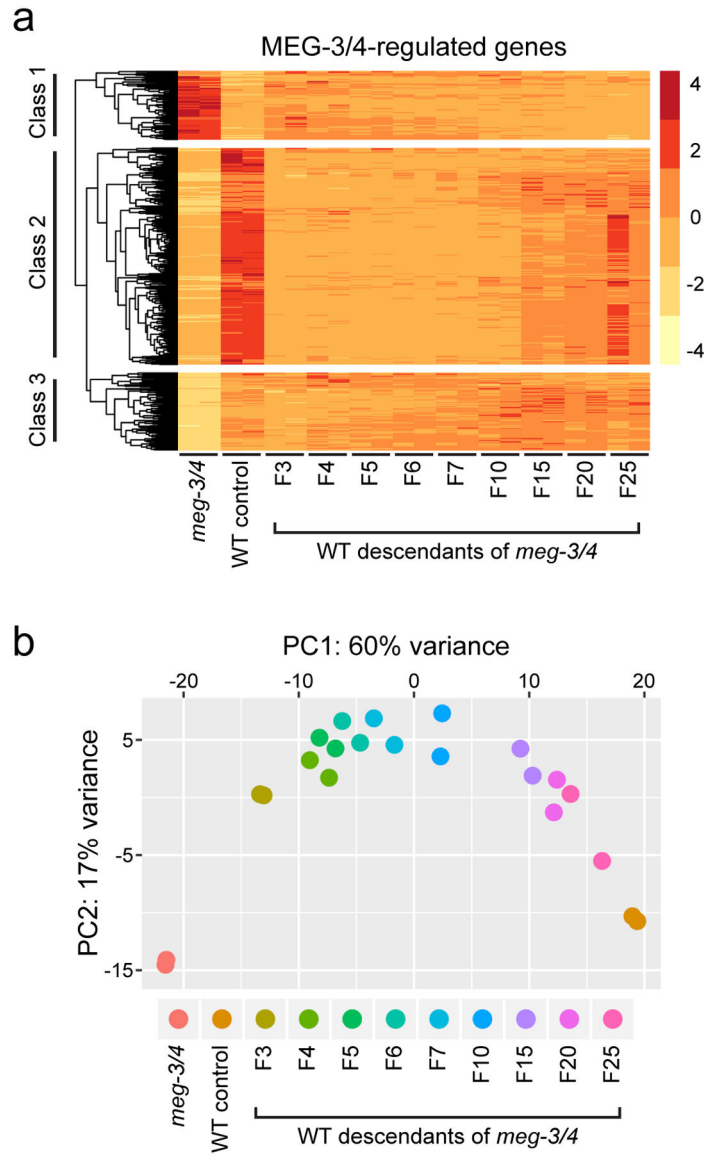
Figure 4. Wild-type descendants of *meg-3/4* inherit aberrant endo-siRNA populations.
(a) Z scores of the levels of endo-siRNAs targeting each MEG-3/4-regulated gene.
Biological replicates were plotted side-by-side for wild type (WT), *meg-3(tm4259) meg-4(ax2026) (meg-3/4)*, and wild-type animals descending from *meg-3/4* mutant animals
(P_0) for the indicated number of generations (F_3-F_{25}). Genes were sorted into groups via
hierarchical clustering (complete linkage method). The three major clusters of endo-siRNAs
are shown and are indicated as Class 1–3. **(b)** Biplot of the top two principal components
(PC1 and PC2) determined by principal component analysis. Points represent individual
small RNA sequencing libraries, which are color-coded by genotype and by generation. Two
biological replicates were analyzed for each genotype and each generation. Each PC
represents a source of variation, and the distribution of points along a given PC axis
indicates the degree of correlation between libraries for that PC. Note: PC1 explains most of
the variation in the sequencing data. Prior to PCA, read counts were subjected to a
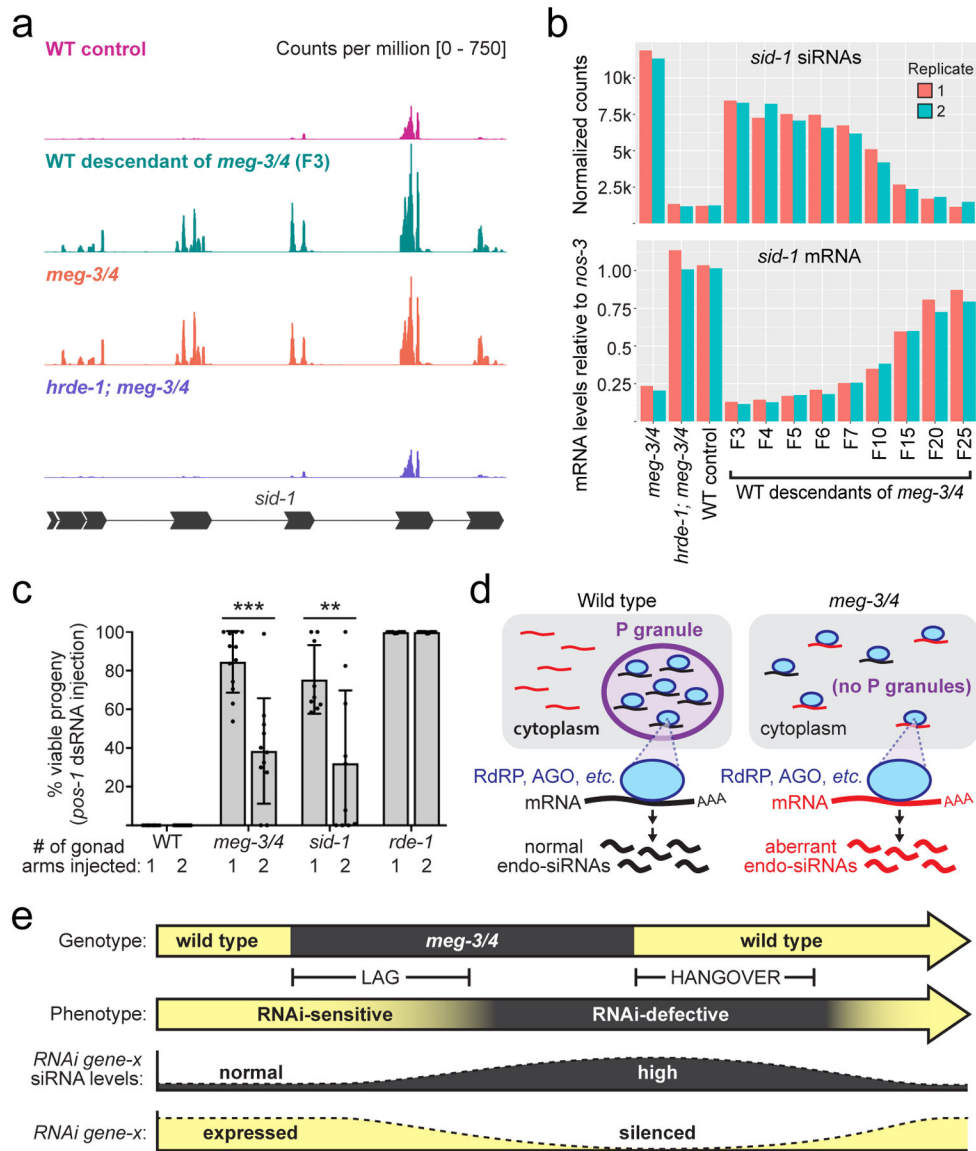
regularized log transformation using the rlog function in DESeq2 (Love et al. 2014). See also Figure S4.

Figure 5. Ancestral loss of P granules is associated with heritable changes in *sid-1* expression.
(a) endo-siRNAs sequenced from animals of the indicated genotypes (and generations after outcross) that map to the *sid-1* locus. A schematic of the *sid-1* locus is shown below. Counts were normalized to total number of reads. (b) Top panel: endo-siRNA reads mapping to the *sid-1* locus were quantified in replicates and across generations during Rde hangovers. Counts were normalized using the median of ratios method (DESeq2). Replicates are shown in red and blue. k=1000. Bottom panel: qRT-PCR was used to quantify *sid-1* mRNA in the samples shown in the top panel. *sid-1* mRNA values are shown relative to the mRNA values of *nos-3*, a germline-expressed gene. (c) Adults of the indicated genotype were injected with 200 ng/ul of *pos-1* dsRNA in either one or both arms of the germline (n ≥ 9 animals per condition). After 18–22 hours of recovery, animals were allowed to lay eggs and % hatching embryos was scored. Some of the variability observed in *meg-3/4* and *sid-1* animals may be due to the fact that responses of *sid-1* mutants to dsRNA injection change with time post-

injection, and the timescale of this change varies from animal to animal(Wang & Hunter 2017). Error bars represent +/− standard deviations of the mean (gray bars). **, p-value < 0.01; ***, p-value < 0.001 (Student's t-test). WT, wild type. **(d)** Model for initiation of Rde hangovers: P granules coordinate and organize endogenous small interfering RNA (endo-siRNA) biogenesis by concentrating endo-siRNA pathway factors (blue ovals) such as RNA-dependent RNA polymerases (RdRPs) and Argonautes (AGOs) together with the appropriate mRNAs. In the absence of MEG-3/4 and therefore P granules, endo-siRNA pathway factors engage the "wrong" pool of mRNAs (long red lines) and thereby initiate the production of aberrant endo-siRNAs (short red lines). **(e)** Model to explain transgenerational disconnects between *meg-3/4* genotype and phenotype. Upon the loss of MEG-3/4, germ cells begin to produce slightly higher-than-normal levels of endo-siRNAs that target one or more genes required for experimental RNAi (*RNAi gene-x*). Due to the heritable nature of the endo-siRNA pathway, endo-siRNAs targeting *RNAi gene-x* accumulate slowly over generations in the absence of MEG-3/4 (lag). After 5–9 generations of aberrant endo-siRNA production/inheritance, these endo-siRNAs reach a level that causes silencing of *RNAi gene-x*; hence the defect in RNAi. After re-introduction of MEG-3/4, aberrant endo-siRNA pools continue to propagate across generations and continue to silence *RNAi gene-x* in genetically wild-type animals (hangover). Over the course of ten generations, genetic systems reassert their control over endo-siRNA biogenesis, returning endo-siRNA pools to normal. See also Figure S5.

KEY RESOURCES TABLE

REAGENT or RESOURCE	SOURCE	IDENTIFIER
Bacterial and Virus Strains		
Escherichia coli OP50	*Caenorhabditis* Genetics Center (CGC)	RRID:WB-STRAIN:OP50
Escherichia coli HT115(DE3)	CGC	RRID:WB-STRAIN:HT115(DE3)
Ahringer RNAi Libraries in *E. coli* HT115(DE3)	Kamath et al., 2003	RRID:SCR_017064
gfp RNAi clone	Author's laboratory	N/A
Chemicals, Peptides, and Recombinant Proteins		
TRIzol Reagent	Invitrogen	Cat#15596018
T4 RNA Ligase 2, truncated	New England BioLabs	Cat#M0242L
Antarctic Phosphatase	New England BioLabs	Cat#M0289L
T4 Polynucleotide Kinase	New England BioLabs	Cat#M0201L
T4 RNA Ligase 1 (ssRNA Ligase)	New England BioLabs	Cat#M0204L
Critical Commercial Assays		
15% Criterion TBE-Urea Polyacrylamide Gel	Bio-Rad	Cat#3450091
Superscript III First-Strand Synthesis System	Invitrogen	Cat#18080051
iTaq Universal SYBR Green Supermix	Bio-Rad	Cat#1725120
MEGAscript T7 Transcription Kit	Invitrogen	Cat#AM1333
Deposited Data		
Small RNA sequencing	This study	GEO: GSE134683
Experimental Models: Organisms/Strains		
C. elegans: N2 wild type	CGC	N2 Bristol
C. elegans: meg-3(tm4259) meg-4(ax2026) X	(Wang et al., 2014)	JH3225
C. elegans: meg-3(ax3055) meg-4(ax3052) X	(Smith et al., 2016)	JH3475
C. elegans: rde-4(ne301) III	(Tabara et al., 2002)	WM49
C. elegans: mjIs31[pie-1p::gfp::h2b] II	(Ashe et al., 2012)	SX461
C. elegans: mjIs31[pie-1p::gfp::h2b] II; meg-3(tm4259) meg-4(ax2026) X	This study	YY1501
C. elegans: mjIs31[pie-1p::gfp::h2b] II; rde-1(ne219) V	Author's laboratory	YY1568
C. elegans: deps-1(bn124) I	(Spike et al., 2008)	DG3226
C. elegans: hrde-1(tm1200) III	National BioResource Project	YY538
C. elegans: nrde-2(gg091) II	(Guang et al., 2010)	YY502
C. elegans: hrde-1(tm1200) III; meg-3(tm4259) meg-4(ax2026) X	This study	YY1512
C. elegans: nrde-2(gg091) II; meg-3(tm4259) meg-4(ax2026) X	This study	YY1513
C. elegans: dpy-3(e27) X	CGC	CB27
C. elegans: meg-3(tm4259) meg-4(ax2026) dpy-3(e27) X	This study	YY1317
C. elegans: mjIs31[pie-1p::gfp::h2b] II; pgl-1(gg547[pgl-1::3xflag::tagrfp]) IV	This study	YY1514

REAGENT or RESOURCE	SOURCE	IDENTIFIER
C. elegans: *mjIs31[pie-1p::gfp::h2b] II; pgl-1(gg547[pgl-1::3xflag::tagrfp]) IV; meg-3(tm4259) meg-4(ax2026) X*	This study	YY1523
C. elegans: *mjIs31[pie-1p::gfp::h2b] II; hrde-1(tm1200) III; pgl-1(gg547[pgl-1::3xflag::tagrfp]) IV; meg-3(tm4259) meg-4(ax2026) X*	This study	YY1548
C. elegans: *mjIs31[pie-1p::gfp::h2b] II; pgl-1(gg547[pgl-1::3xflag::tagrfp]) IV; dpy-3(e27) X*	This study	YY1549
C. elegans: *mjIs31[pie-1p::gfp::h2b] II; hrde-1(tm1200) III; pgl-1(gg547[pgl-1::3xflag::tagrfp]) IV*	This study	YY1552
C. elegans: *mjIs31[pie-1p::gfp::h2b] II; pgl-1(gg547[pgl-1::3xflag::tagrfp]) IV; meg-3(tm4259) meg-4(ax2026) dpy-3(e27) X*	This study	YY1553
C. elegans: *sid-1(qt9) V*	(Winston et al., 2002)	HC196
C. elegans: *rde-1(ne219) V*	(Tabara et al., 1999)	WM27
Oligonucleotides		
nos-3 mRNA Forward: 5' GGAGGCTATCGGCAGTATCA 3'	This study	N/A
nos-3 mRNA Reverse: 5' GTGGCCCTGCTTGAGGATTA 3'	This study	N/A
rde-11 mRNA Forward: 5' GATTTCGGACTCCCTATGTGGAC 3'	This study	N/A
rde-11 mRNA Reverse: 5' GTAGAGATACAGTCCGTCCAGC 3'	This study	N/A
sid-1 mRNA Forward: 5' CGGCGAATGAATCCATCTAT 3'	This study	N/A
sid-1 mRNA Reverse: 5' CGGGAGCTATGAAGACGAAG 3'	This study	N/A
Software and Algorithms		
cutadapt 1.14	(Martin, 2011)	RRID:SCR_011841
Bowtie 1.2.2	(Langmead et al., 2009)	RRID:SCR_005476
featureCounts	(Liao et al., 2014)	RRID:SCR_012919
RStudio	(RStudio Team, 2016)	RRID:SCR_000432
DESeq2 1.22.2	(Love et al., 2014)	RRID:SCR_015687
pheatmap 1.0.12	(Kolde, 2015)	RRID:SCR_016418
DEGreport 1.18.1	(Pantano, 2019)	N/A
deepTools 3.0.2	(Ramírez et al., 2016)	RRID:SCR_016366
Sushi 1.20.0	(Phanstiel et al., 2014)	N/A
ZEN Digital Imaging for Light Microscopy	Zeiss	RRID:SCR_013672
Fiji	(Schindelin et al., 2012)	RRID:SCR_002285
Other		
Axio Observer.Z1 microscope	Zeiss	N/A
ORCA-Flash 4.0 CMOS camera	Hamamatsu	N/A
Plan-Apochromat 63×/1.4 Oil DIC M27 objective	Zeiss	N/A
Plan-Apochromat 20×/0.8 M27 objective	Zeiss	N/A
EC Plan-Neofluar 10×/0.3 Ph1 M27 objective	Zeiss	N/A